

Dalton Transactions

Accepted Manuscript



This is an *Accepted Manuscript*, which has been through the Royal Society of Chemistry peer review process and has been accepted for publication.

Accepted Manuscripts are published online shortly after acceptance, before technical editing, formatting and proof reading. Using this free service, authors can make their results available to the community, in citable form, before we publish the edited article. We will replace this *Accepted Manuscript* with the edited and formatted *Advance Article* as soon as it is available.

You can find more information about *Accepted Manuscripts* in the [Information for Authors](#).

Please note that technical editing may introduce minor changes to the text and/or graphics, which may alter content. The journal's standard [Terms & Conditions](#) and the [Ethical guidelines](#) still apply. In no event shall the Royal Society of Chemistry be held responsible for any errors or omissions in this *Accepted Manuscript* or any consequences arising from the use of any information it contains.

ARTICLE

Peripheral substitution as a tool for tuning electron-accepting properties of phthalocyanine analogs in intramolecular charge transfer

Antonin Cidlina,^a Veronika Novakova,^{*b} Miroslav Miletin^a and Petr Zimcik^{*a}

Cite this: DOI: 10.1039/x0xx00000x

Received 00th January 2012,
Accepted 00th January 2012

DOI: 10.1039/x0xx00000x

www.rsc.org/

The intramolecular charge transfer (ICT), which is a pathway for excited state relaxation, was studied on the newly synthesized zinc (II) complexes of tetrapyrrolineporphyrins bearing one fixed donor (i.e., a dialkylamino substituent). The rest of the peripheral substituents on the core were designed with respect to their different electronic effects (OBu, neopentyl, *t*Bu, COOBu). The photophysical (singlet oxygen and fluorescence quantum yields) and electrochemical (reduction potentials) properties were determined and compared within the series and with compounds that did not contain a donor moiety. The ICT efficiency correlated well with both the electron-deficient character of the core and the Hammett substituent constants σ_p . The most efficient ICT was observed for the core with the most electron-accepting substituent (COOBu), and the lowest ICT efficiency was detected for the least electron-deficient core (substituted by OBu). Titration of DMSO solutions of target compounds with H₂SO₄ indicated that basicity of the azomethine bridges was largely influenced by character of the peripheral substituents while the dialkylamino donor center remained nearly unaffected. Further, protonation of donor nitrogen caused partial restoration of fluorescence quantum yield (increase up to 90 times) due to blocking of ICT. The results implied that the ICT efficiency was strongly dependent on the electron-accepting properties of the core whose properties can be readily affected by suitable selection of peripheral substituents.

Introduction

Azaphthalocyanines are aza-analogues of phthalocyanines (Pcs) where the benzene rings are replaced by nitrogen heterocycles. The most studied class of these compounds are the tetrapyrrolineporphyrins (TPyzPzs). TPyzPzs are well-known synthetic dyes with outstanding photophysical, photochemical and electrochemical properties.¹⁻⁴ TPyzPzs exhibit a sharp absorption Q band above 650 nm. If they are suitably substituted or coordinate specific central cations, TPyzPzs exhibit high quantum yields of singlet oxygen or fluorescence.⁵ TPyzPzs can be advantageously used in various application, such as photosensitizers for photodynamic therapy,⁶ catalysts,⁷ non-linear optical materials,⁸ liquid crystals⁹ or crystals with large voids.¹⁰ The presence of nitrogen atoms in the TPyzPz core imparts more electron-deficient character to the entire macrocycle compared to the parent Pcs.¹¹ Therefore, TPyzPzs substituted with electron donors (e.g., amines) undergo ultrafast intramolecular charge transfer (ICT) that quenches the excited state in TPyzPzs.¹² The ICT only occurs in the presence of at least one donor (typically amine) in conjugation with the macrocycle core, which serves as an acceptor. The ICT can be blocked by various factors that may

switch fluorescence between ON and OFF states and can be used for the development of sensors for different analytes (e.g., pH sensors¹³ or sensors sensitive to metal cations¹⁴).

Recent results have indicated that the ICT efficiency may be primarily influenced by the type of macrocycle (Pc, TPyzPz)¹¹ or the electron-donating properties of the donor.¹⁵ The current study is focused on the impact of the electronic properties of the substituents on the TPyzPz core because they may affect electron-deficient properties of the core and consequently the feasibility of the whole ICT process. Therefore, TPyzPzs **1Zn-5Zn** (Chart 1) were designed and synthesized. The donor center and central metal of the target TPyzPzs were fixed. Only one donor center was considered in the study to detect small differences between target compounds. ICT in TPyzPzs is very strong and all photophysical parameters of interest are approaching zero if two or more donor centers are introduced.¹² The rest of TPyzPz core was decorated by substituents with different electronic effects. The selection of the substituents was carried out with the respect to their different Hammett substituent constants σ_p .¹⁶ Simultaneously, these substituents were also selected based on their effect on the inhibition of aggregation to eliminate non-specific quenching of excited states (i.e., non-ICT related).

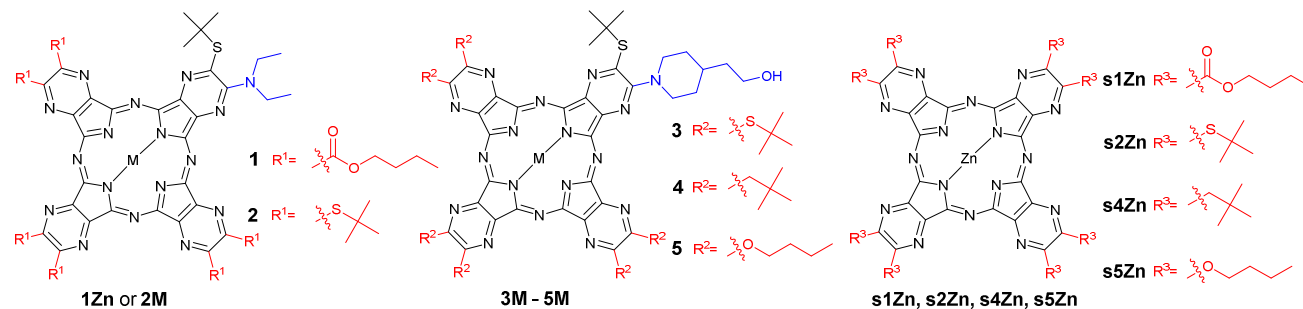


Chart 1 Structures of investigated compound. M = Zn or 2H.

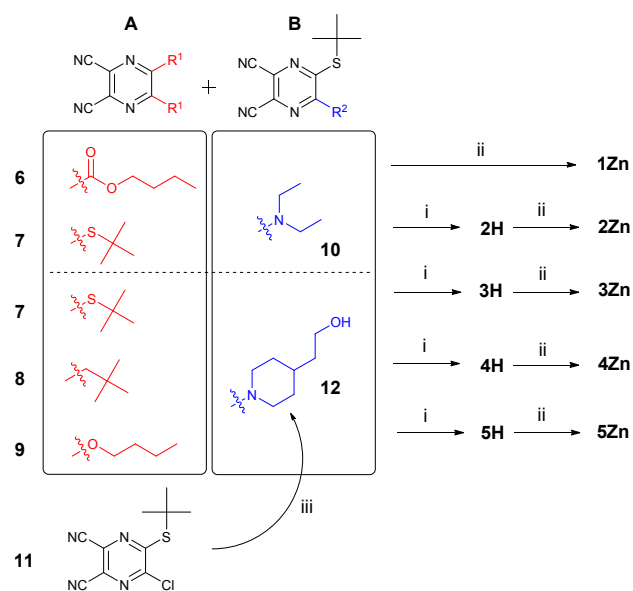
Results and discussion

Synthesis

In general, the synthesis of TPzPzs starts from the corresponding precursors, which are substituted pyrazine-2,3-dicarbonitriles. The synthesis of most of the precursors (**6** – **11**)^{12, 14, 17-20} (Scheme 1) was performed according to previously published protocols. Precursor **12** was obtained nearly quantitatively by nucleophilic substitution of chlorine in **11** by 2-(piperidin-4-yl)ethan-1-ol as a nucleophilic agent in the presence of K₂CO₃ serving as a base. The statistical condensation of two different precursors (A and B, Scheme 1) in a 3 : 1 ratio was used for the synthesis of unsymmetrical TPzPzs. The reaction led to the formation of a mixture of six different congeners (i.e., AAAA, AAAB, AABB, ABAB, ABBA and BBBB) from which the AAAB type was chromatographically separated. The selection of the donor moiety (i.e. precursor B, **10** or **12**) for the reaction was driven by the hydrophobicity of the precursor A. For hydrophobic precursors **7** - **9**, more hydrophilic partner for cyclotetramerization **12** substantially simplified the chromatographic isolation of the target AAAB type congener. However, less hydrophobic **6** required precursor **10** for successful isolation of target TPzPz **1Zn** because the use of **12** yielded an inseparable mixture of congeners with nearly the same migration on silica. Being distant from the amine, the hydroxyl group in the donor part of macrocycles **3Zn**-**5Zn** was not expected to influence the photophysical behavior of the donor. However, to confirm this premise, TPzPz **2Zn** with the same peripheral substituents as **3Zn** but a different donor part was synthesized.¹² As can be seen later on in detail in this work, studied properties of **2Zn** and **3Zn** were similar and confirmed the relevance of our hypothesis.

The cyclotetramerization of precursors **7** - **9** with **10** or **12** was initiated by magnesium butoxide. The statistical mixture of six congeners of the magnesium complexes was difficult to separate due to strong tailing of the compounds on silica. The treatment of the statistical mixture of magnesium complexes with *p*-toluenesulfonic acid (TsOH) in THF at room temperature afforded a mixture of metal-free complexes that typically do not tail. In addition, their isolation has been reported to be more efficient.¹² Indeed, the conversion of the

mixture of magnesium derivatives to metal-free derivatives significantly facilitated the separation, and AAAB type congeners **2H** - **5H** were isolated in yields ranging from 9 % to 16 %. Zinc complexes **2Zn** - **5Zn** were prepared from corresponding metal-free derivatives **2H** - **5H** by reaction with anhydrous zinc acetate in pyridine under reflux (Scheme 1). The use of a butoxide initiator for the synthesis of **1H** (and subsequently **1Zn**) failed, and only dark decomposition products were obtained upon treatment of **6** with **10** (or **12**) with magnesium butoxide. Therefore, the synthesis of **1Zn** was performed using the metal ion template method with anhydrous zinc acetate in anhydrous DMF or pyridine (Scheme 1). The use of pyridine as the solvent in the template synthesis appeared to be more advantageous than DMF because fewer side products were produced. Despite this fact, the isolated yield of **1Zn** was only 0.6 %. This low yield is due to both the lower efficiency of the template cyclotetramerization method (synthesis of symmetrical **s1Zn** is reported to be only 13% by template method¹⁷) and the necessity of separation of the congeners as the zinc complexes. The congeners strongly tailed



Scheme 1 Reaction conditions: (i) a) Mg(BuO)₂, butanol, reflux, 7 h; b) TsOH, THF, rt, 1 h; (ii) Zn(CH₃COO)₂, pyridine, reflux, 1 h; (iii) 2-(piperidin-4-yl)ethan-1-ol, K₂CO₃, DMSO, rt.

on silica (Figure S1) and the pure fractions were isolated after number of chromatography repetitions that substantially decreased the final yield. For comparison in the photophysical measurements, the corresponding symmetrical compounds **s1Zn**, **s2Zn**, **s4Zn** and **s5Zn** (Chart 1) without a donor dialkylamino substituent were prepared according to published procedures.¹⁷⁻²⁰

Electrochemistry

The TPzPz macrocycle in the ICT behaves as an acceptor of electrons, and therefore, a half-wave potential of the first reduction (E_{red}^1) may indicate feasibility of the process. The electrochemistry of the target compounds was investigated *via* cyclic and square wave voltammetry in THF at room temperature with ferrocene as an internal standard. The half-wave potentials were obtained from the square wave voltammetry, and the data are listed in Table 1.

Table 1 Electrochemical data of the studied compounds in THF [a].

	σ_p [b]	E_{ox} (V)	E_{red}^1 (V)	E_{red}^2 (V)
1Zn [c]	0.45 (COOEt)	1.50	-0.33	-0.69
2Zn	0.07 (SCHMe ₂)	1.03	-0.79	-1.21
3Zn	0.07 (SCHMe ₂)	1.02	-0.77	-1.19
4Zn	-0.17 (CH ₂ CMe ₃)	1.09	-0.78	-1.18
5Zn	-0.32 (OBu)	0.67	-0.83	-1.28
s1Zn [d]	0.45 (COOEt)	1.40	-0.34	-0.60
s2Zn	0.07 (SCHMe ₂)	1.10	-0.78	-1.08
s4Zn	-0.17 (CH ₂ CMe ₃)	1.14	-0.88	-1.18
s5Zn	-0.32 (OBu)	0.68	-0.96	-1.30

[a] The potentials E_{red}^1 , E_{red}^2 , E_{red}^3 and E_{ox} are expressed as $E_{1/2}$ (in V vs. SCE) with Fc/Fc^+ as the internal standard; [b] Hammett substituent constant of the closest available peripheral substituent.¹⁶ [c] E_{red}^3 (V) = -1.48 [d] E_{red}^3 (V) = -1.29

All of the studied compounds (**1Zn** - **5Zn** and **s1Zn**, **s2Zn**, **s4Zn** and **s5Zn**) were characterized by at least two reductions in the electrochemical window provided by the solvent. Three reductions were observed for **1Zn** and **s1Zn**. Compounds **2Zn** and **3Zn**, which have a very similar peripheral substitution pattern, had very close reduction potentials, confirming the limited influence of the hydroxy substituent in **3Zn** on the electrochemical properties. The values of E_{red}^1 correlated well with the Hammett substituent constants σ_p of the peripheral substituents irrespective of whether the TPzPz was substituted with a donor (Figure 1). Therefore, the most electron-deficient TPzPz core ($E_{\text{red}}^1 \sim -0.33$ V vs. SCE) was observed for **1Zn** and **s1Zn** with the strongest electron-withdrawing COOBu substituents. On the other hand, the most electron-donating OBU substituents provided a core with weak electron-accepting properties, and **5Zn** and **s5Zn** had the most negative E_{red}^1 values (Table 1).

To obtain a complete data set, the oxidation processes were also investigated. One irreversible oxidation was observed for all of the molecules. The oxidation potential (E_{ox}) followed a trend to that of the reduction potential. A decrease in E_{ox} from

1.50 V vs. SCE (**1Zn**) to 0.67 V vs. SCE (**5Zn**) was observed as the Hammett substituent constant σ_p decreased from 0.45 to -0.32 for all studied compounds irrespective of the presence or absence of a donor (Table 1). Therefore, the Hammett substituent constants σ_p of the peripheral substituents are useful tools for the prediction of the electron-accepting properties of the entire TPzPz core.

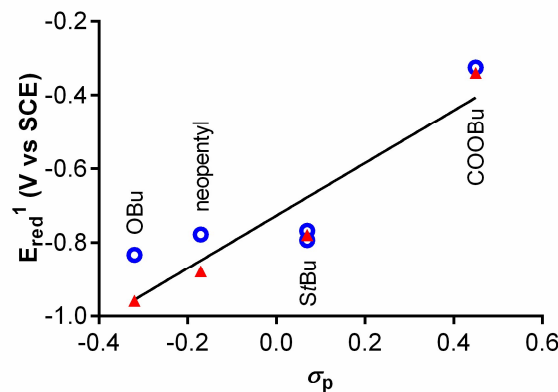


Fig. 1 Dependence of the E_{red}^1 value of the studied compounds and the Hammett substituent constants σ_p . Blue dots: compounds **1Zn** - **5Zn** with donor, red triangles: compounds **s1Zn**, **s2Zn**, **s4Zn** and **s5Zn** without a donor.

Absorption spectra

The absorption spectra were measured in THF. The absorption spectra of target zinc complexes exhibited characteristic bands in the range of 350 nm to 377 nm for the high energy B-band and 618 nm to 652 nm for the low energy Q-band (Table 2). The Q-bands of all of the compounds had an unsplit sharp shape with well-resolved vibrational bands (Figure 2), which indicates the presence of the monomeric form of the compounds in the solution without any aggregates. The Q-band of **1Zn** was significantly broader than that for the other compounds. However, the spectrum did not change in shape or extinction coefficient for a wide range of concentrations (from 0.8 μM to 100 μM , Figure S2). In addition, an increasing temperature did not alter the spectrum, which confirmed the presence of only the monomeric form in solution. The position of the absorption maxima of the Q-band was sensitive to changes in the peripheral substitution. The contribution of peripheral substituents to the bathochromic shift increased in the order OBU < neopentyl < SiBu ~ COOBu for both series of TPzPzs with or without the donor. The hydroxy substituent in the alkyl chain of **3Zn** did not alter the shape of the spectrum that was only insignificantly red-shifted by 1 nm from **2Zn** (Figure 2). Of note, the hydroxy group in Pcs was reported to form intermolecular coordinating bond to central zinc of next macrocycle thus forming highly stable J-dimers with modified Q-band shape.^{21, 22} No such observations were made for **3Zn** and its absorption spectrum perfectly overlapped the one of **2Zn**.

Table 2 Absorption and photophysical properties of investigated compounds in THF and DMSO^[a].

	Q-band λ_{\max} (nm)	λ_{em} (nm)	$\Delta\lambda$ (cm ⁻¹)	$\Phi_{\text{F}}^{\text{[b]}}$	$\Phi_{\Delta}^{\text{[b]}}$	$\Phi_{\text{F}} + \Phi_{\Delta}$	Φ_{F} (DMSO)	$\Phi_{\text{F}}^{\text{(max)}}$ (DMSO + H ⁺) ^[c]	Increase of Φ_{F} (DMSO) ^[d]
1Zn	652	670	412	0.001	0.02	0.02	0.001	0.089	89
2Zn	651	658	163	0.02	0.19	0.21	0.001	0.01	10
3Zn	650	658	187	0.04	0.22	0.25	0.002	0.01	5
4Zn	639	652	312	0.02	0.19	0.21	0.001	0.01	10
5Zn	626	633	177	0.06	0.31	0.37	0.002	0.006	3
s1Zn	648	657	211	0.27	0.55	0.82	0.17		
s2Zn	650	656	141	0.32	0.51	0.83	0.15		
s4Zn	636	642	147	0.29	0.54	0.83	0.22		
s5Zn	618	624	156	0.32	0.53	0.85	0.22		

^[a] Absorption maximum (λ_{\max}), emission maximum (λ_{em}), Stokes shift ($\Delta\lambda$), quantum yield of fluorescence (Φ_{F}), quantum yield of singlet oxygen (Φ_{Δ}). The data are obtained in THF unless otherwise indicated. ^[b] mean of three independent measurements, estimated error $\pm 15\%$. ^[c] maximum Φ_{F} value in protonation experiments with H₂SO₄. ^[d] calculated as follows: $\Phi_{\text{F}}^{\text{(max)}} / \Phi_{\text{F}}$ (in DMSO).

The presence of the donor amino substituent in **1Zn** - **5Zn** induced a small red shift compared to the corresponding symmetrical compounds without the amino substituent (Table 2). This result is in good agreement with the literature results for the amino substituent, which was reported to contribute to the bathochromic shift of TPzPz and related compounds. It can be explained by participation of the lone pair of electrons on the nitrogen on the π -system of the macrocycle.²⁰

The metal-free complexes (Figure S3 in Supporting Information) exhibited the characteristic splitting of the Q-band caused by the two hydrogens occupying the central pyrrole nitrogens, reducing the molecular symmetry from D_{4h} to D_{2h} .²³ The typical absorption bands of metal-free TPzPz in the range from app. 430 nm to 500 nm may be due to $n-\pi^*$ transitions from the lone pairs of the pyrroline nitrogens.¹²

intersystem crossing channels.¹² Therefore, the determination of the photophysical parameters may indicate the efficiency of the ICT. The photophysical parameters were determined for only the zinc complexes because the metal-free TPzPz typically have weak Φ_{F} and Φ_{Δ} values due to other relaxation channels for the excited state. Therefore, these compounds are not suitable for investigation of the ICT efficiency.⁵ The fluorescence measurements were performed in THF after excitation at the Q-band ($\lambda_{\text{exc}} = 600$ nm). The shape of the emission spectra was typical for TPzPz and related compounds with a mirror image of the absorption Q-band and a small Stokes shift (Figures 3 and S4, Table 2). The excitation spectra were also collected (Figure S4), and their perfect match with the absorption spectra confirmed the presence of only the monomeric form for all of the studied TPzPz (both unsymmetrical and symmetrical). Therefore, the photophysical data were not affected by aggregation.

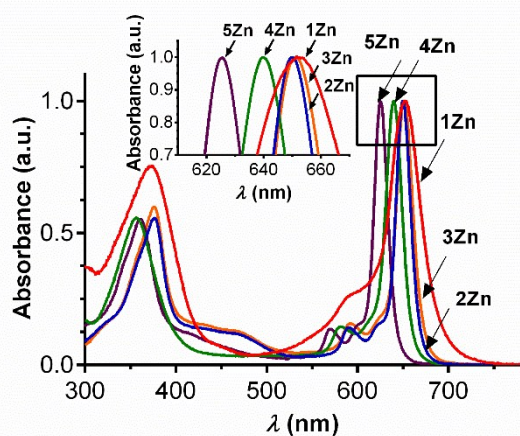


Fig. 2 Normalized absorption spectra of **1Zn** (red), **2Zn** (blue), **3Zn** (orange), **4Zn** (green) and **5Zn** (purple) in THF. Inset: Enlarged part of the Q-band area.

Fluorescence and singlet oxygen production

The ICT is a competitive relaxation process of the singlet excited state and is typically reducing the fluorescence or

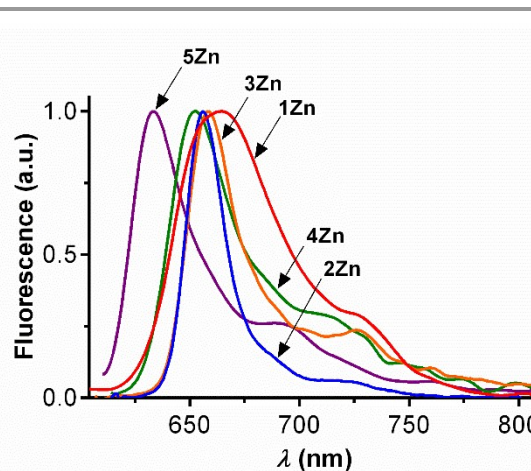


Fig. 3 Normalized emission spectra of **1Zn** (red), **2Zn** (blue), **3Zn** (orange), **4Zn** (green) and **5Zn** (purple) in THF. The spectra were corrected for the instrument response.

The fluorescence quantum yields (Φ_F) were determined in THF with unsubstituted zinc phthalocyanine (ZnPc, $\Phi_{F(\text{THF})} = 0.32^5$) as the reference (Table 2). The Φ_F of symmetrical compounds without any donor (**s1Zn**, **s2Zn**, **s4Zn** and **s5Zn**) achieved comparable values close 0.30, which is typical for zinc complexes of TPyzPzs and Pcs.^{4, 24} However, the fluorescence channel was more than one order of magnitude weaker for the compounds bearing an amine donor center, and for example, the fluorescence of compound **1Zn** bearing butoxycarbonyl substituents was barely detected.

The quantum yields of singlet oxygen (Φ_Δ) were determined in THF using a singlet oxygen quencher 1,3-diphenylisobenzofuran (DPBF) with unsubstituted ZnPc ($\Phi_{\Delta(\text{THF})} = 0.53^{25}$) as a reference. The data are summarized in Table 2 and followed a trend similar to that observed for the fluorescence data. The symmetrical compounds without any donor produced singlet oxygen at a high rate, and their Φ_Δ values were determined to be more than 0.50, which is typical for zinc complexes of TPyzPzs and Pcs.^{26, 27} The Φ_Δ values were significantly lower for compounds **1Zn** – **5Zn**, which contained a donor center, where the lowest value ($\Phi_\Delta = 0.02$) was obtained for **1Zn**.

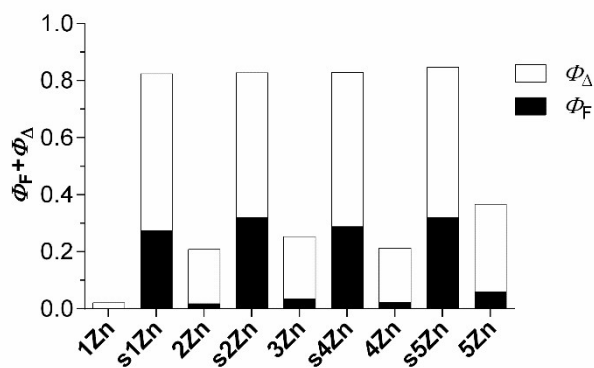


Fig. 4 Comparison of the sums of Φ_F (full columns) and Φ_Δ (blank columns) for **1Zn** – **5Zn** with corresponding symmetrical molecules **s1Zn**, **s2Zn**, **s4Zn**, and **s5Zn**.

Fluorescence emission and intersystem crossing to a triplet state are two most important deactivation pathways of singlet excited states. Because the quenching of the triplet state of zinc Pcs and their analogues by oxygen is typically 100% in organic solvents,²⁸⁻³⁰ the Φ_Δ values may serve as an indicator of intersystem crossing.¹⁵ Therefore, the sum of $\Phi_\Delta + \Phi_F$ covers the most important pathways if no other processes (e.g., ICT) occur. The sum is typically constant for various macrocycles even though the ratio between the fluorescence and singlet oxygen production may vary depending on various structural factors (e.g., heavy atom effect).^{31, 32} This fact was confirmed also in the current study for symmetrical **s1Zn**, **s2Zn**, **s4Zn** and **s5Zn**. Their sum of $\Phi_\Delta + \Phi_F$ reached comparable values (approximately of 0.83). The ratio between the two deactivation processes, Φ_Δ and Φ_F , slightly varied (Figure 4, Table 2). This observation also confirmed that the photophysics of compounds

without a donor were not affected by any extraordinary deactivation pathway.

On the other hand, ICT induced a significant decrease in the sum of $\Phi_\Delta + \Phi_F$ in compounds bearing a donor center (**1Zn** – **5Zn**). The ICT efficiency followed the trend **1Zn** > **2Zn** ~ **3Zn** ~ **4Zn** > **5Zn**. The presence of the hydroxyl substituent in the donor moiety did not substantially affect the photophysical properties (Table 2), and the sum of $\Phi_\Delta + \Phi_F$ for **2Zn** and **3Zn** was determined to be comparable.

The ICT efficiency correlated well with the value of the Hammett substituent constant σ_p of the peripheral substituents. A decrease in the ICT efficiency with the change of the electronic properties of the peripheral substituents from electron withdrawing to electron donating was observed (Figure 5). The electronic effects apparently substantially influenced the electron-deficient character of the TPyzPz core as well as its ability to behave as an acceptor in ICT. To gain further insight, the photophysical data were directly correlated with the electrochemical data. Indeed, the values of E_{red}^1 (Table 1) correlated with the efficiency of the ICT expressed as a sum of Φ_F and Φ_Δ (Figure 5). The most efficient ICT process was present in the TPyzPz core, which possessed the most electron-deficient character (**1Zn**), and low ICT efficiency was observed for the least electron-deficient core of **5Zn**.

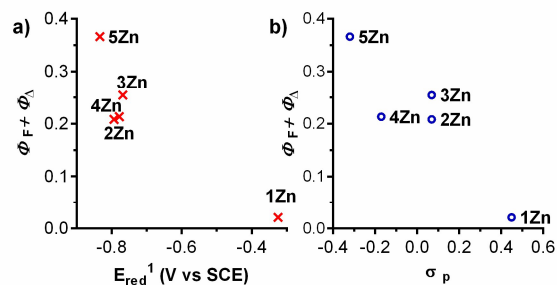


Fig. 5 Influence of the sum of quantum yields on E_{red}^1 values (a) and the Hammett substituent constants of the peripheral substituents σ_p (b) of **1Zn** – **5Zn**.

Protonation of nitrogens

Protonation of the donor nitrogen in ICT has been previously shown to lead to restoration (full or partial) of the photophysical properties (e.g. fluorescence).^{12, 33, 34} In order to demonstrate this effect after blocking of the ICT, the fluorescence was monitored as a function of the sulfuric acid concentration in DMSO. THF was found unsuitable for this experiment as it decomposed at higher sulfuric acid concentrations. It must be noted that besides the donor nitrogen, the azomethine nitrogens in TPyzPz can be also protonated and protonation at this site was reported to considerably decrease the Φ_F values for TPyzPz and Pc.^{12, 35, 36}

In order to distinguish between the changes in fluorescence intensity induced by protonation at different sites (azomethine × donor nitrogen), the experiment with sulfuric acid was performed first with **s1Zn**, **s2Zn**, **s4Zn** and **s5Zn** (Figure 6a,

Figure S6). Their Φ_F values in pure DMSO were lower than in THF but still comparable (Table 2). A decrease of Φ_F was observed for all compounds at higher concentrations of sulfuric acid and was accompanied by typical changes in absorption spectra³⁶ indicating protonation of one azomethine nitrogen (Figure S5). The progress of the changes (Figure 6a) was influenced by basicity of these nitrogens that reflected well the electronic properties of the substituents, i.e. basicity was decreasing in order **s5Zn** (electron-donating) > **s2Zn** ~ **s4Zn** > **s1Zn** (electron-withdrawing). The Φ_F values of compounds with the donor center **1Zn**–**5Zn** in DMSO were extremely low (typically below 0.002, Table 2) as a consequence of high efficiency of ICT in this polar solvent.^{12, 37} The titrations with sulfuric acid had clearly biphasic character (Figure 6b). The initial increasing phase due to protonation of the donor nitrogen was followed by decrease of the Φ_F values due to protonation of the azomethine nitrogen. Interestingly, the “break point” where the decrease of fluorescence prevailed was largely influenced by basicity of the azomethine nitrogens and corresponded well with the basicity of the compounds without any donor. For example, the most basic **5Zn** was protonated on the azomethine nitrogens at low concentrations of acid and that is why its “break point” appeared already at ~ 13% of sulfuric acid in DMSO (v/v) and the maximum increase in Φ_F values was only ~3 times. On the other hand, the least basic core of **1Zn** allowed almost full protonation of the donor center (“break point” at ~33%, increase in Φ_F values ~90 times) before the protonation of azomethine nitrogen substantially decreased the Φ_F value. Interestingly, the basicity of the donor center was almost not influenced as deduced from the progress of initial increasing phase (Figure 6b, inset) that was very similar for all compounds, no matter of peripheral substituents. These experiments unequivocally demonstrated that ICT in target compounds can be blocked by protonation of the donor center.

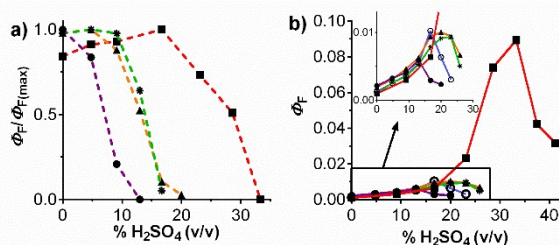


Fig. 6. Changes of normalized Φ_F values of studied TPyzPzs (1 μ M) in DMSO after addition of sulfuric acid. a) **s1Zn** (square, red dashed line), **s2Zn** (triangle, orange dashed line), **s4Zn** (asterisk, green dashed line), **s5Zn** (dot, magenta dashed line). b) **1Zn** (square, red full line), **2Zn** (circle, blue full line), **3Zn** (triangle, orange full line), **4Zn** (asterisk, green full line), **5Zn** (dot, magenta full line).

Conclusion

Target compounds **1Zn** – **5Zn** bearing one donor moiety for ICT represented by the dialkylamino substituent were synthesized using a statistical condensation of two different precursors. The ICT substantially quenched both the fluorescence and singlet oxygen production compared to the

corresponding molecules without the donor moiety (i.e., **s1Zn**, **s2Zn**, **s4Zn** and **s5Zn**). The efficiency of the ICT significantly depended on the electron-deficient character of the acceptor (TPyzPz core). The highest efficiency of ICT was observed for the compound bearing electron-withdrawing peripheral substituents with the most positive σ_p value. The electron-accepting properties of the core can be easily tuned by suitable selection of peripheral substituents. The selection of the substituents can be based on the Hammett substituent constant σ_p , which allows for estimation of the electron-deficient properties of the core. The experiments with protonation of different macrocycle sites indicated that basicity of the azomethine nitrogens can be largely influenced by character of the peripheral substituents while the dialkylamino donor center remains nearly unaffected. Partial restoration of the Φ_F after protonation confirmed a key role of the donor lone pair in ICT process. These relationships along with previously discovered effects of the donor properties¹⁵ and the type of the macrocycle¹¹ can be used for the rational design of new fluorescence molecular sensors.

Experimental

All of the organic solvents used in the syntheses were of analytical grade. Anhydrous butanol for the cyclotetramerization was freshly distilled from magnesium, and anhydrous DMF and anhydrous pyridine were purchased from Sigma-Aldrich. Unsubstituted zinc phthalocyanine (ZnPc) was purchased from Sigma-Aldrich. All of the other chemicals for the syntheses were purchased from certified suppliers (i.e., Sigma-Aldrich, TCI Europe, Acros, and Merck) and used as received. TLC was performed on Merck aluminum sheets coated with silica gel 60 F254. Merck Kieselgel 60 (0.040–0.063 mm) was used for column chromatography. The melting points were measured on an Electrothermal IA9200-series digital melting-point apparatus (Electrothermal Engineering, Southend-on-Sea, Essex, Great Britain). The infrared spectra were measured on a Nicolet 6700 spectrometer in ATR mode. The ¹H and ¹³C NMR spectra were recorded on a Varian Mercury Vx BB 300 NMR spectrometer or VNMR S500 NMR spectrometer. The chemical shifts are reported relative to Si(CH₃)₄ and were locked to the signal of the solvent. Elemental analyses were performed on an Automatic Microanalyser EA1110CE (Fisons Instruments, Milan, Italy). The UV–Vis spectra were recorded using a Shimadzu UV-2600 spectrophotometer. The steady-state fluorescence spectra were measured using an AMINCO-Bowman Series 2 luminescence spectrometer. The MALDI-TOF mass spectra were recorded in positive reflectron mode on a 4800 MALDI TOF/TOF mass spectrometer (AB Sciex, Framingham, MA, USA) in trans-2-[3-(4-tertbutylphenyl)-2-methyl-2-propenylidene]-malononitrile, which was used as a matrix. The instrument was calibrated externally with a five-point calibration using a Peptide Calibration Mix1 kit (LaserBio Laboratories, Sophia-Antipolis, France). High resolution mass spectra (HR MS) were measured using a UHPLC system Acquity UPLC I-class

(Waters, Millford, USA) coupled to a high resolution mass spectrometer Synapt G2Si (Waters, Manchester, UK) based on Q-TOF. The chromatography for this HR MS measurement was performed using an Acquity UPLC BEH300 C4 (2.1 × 50 mm, 1.7 μm) column with isocratic elution consisting of acetonitrile and 10 mM ammonium formate buffer at a pH of 3 (90:10) and a flow rate of 0.4 mL/min. Electrospray ionization was operated in positive mode. The ESI spectra were recorded in the range 200 - 2000 *m/z* using glu-fibrinopeptide B as a lock mass reference and sodium iodide for calibration. Precursors dibutyl 5,6-dicyanopyrazine-2,3-dicarboxylate (**6**),¹⁷ 5,6-bis(*tert*-butylsulfanyl)pyrazine-2,3-dicarbonitrile (**7**),¹⁹ 5,6-dineopentylpyrazine-2,3-dicarbonitrile (**8**),²⁰ 5,6-dibutoxypyrazine-2,3-dicarbonitrile (**9**),¹⁸ 5-(*tert*-butylsulfanyl)-6-(diethylamino)pyrazine-2,3-dicarbonitrile (**10**),¹² 5-(*tert*-butylsulfanyl)-6-chloropyrazine-2,3-dicarbonitrile (**11**),¹⁴ TPyzPz **2Zn**¹² and symmetrical TPyzPzs **s1Zn**,¹⁷ **s2Zn**,¹⁹ **s4Zn**²⁰ and **s5Zn**¹⁸ were prepared according to published procedures.

5-(*tert*-butylsulfanyl)-6-[4-(2-hydroxyethyl)piperidin-1-yl]pyrazine-2,3-dicarbonitrile (**12**)

Finely ground anhydrous potassium carbonate (213 mg, 1.54 mmol) was sonicated in DMF (15 mL) for 15 min, and then, 2-(piperidin-4-yl)ethan-1-ol (180 mg, 1.39 mmol) was added. The mixture was stirred for 10 min at rt, and the solution of compound **11** (260 mg, 1.03 mmol) in DMF (3 mL) was added dropwise. The reaction was completed immediately according to TLC using ethyl acetate as the mobile phase. The mixture was concentrated under reduced pressure, and water was added. The mixture was extracted with ethyl acetate (3 × 15 mL). The combined organic layers were dried (Na₂SO₄), and the solvent was evaporated under reduced pressure. The compound was further purified using column chromatography on silica with chloroform/ethyl acetate (1:1) as the eluent. The pure product was recrystallized from methanol. Yield 345 mg (97 %) of yellow solid; mp 139.8 – 140.5 °C. Found: C, 59.39; H, 6.78; N, 20.56. Calcd. for: C₁₇H₂₃N₅OS: C, 59.10; H, 6.71 N, 20.27 %. $\nu_{\max}/\text{cm}^{-1}$ 3503, 2993, 2960, 2942, 2917, 2805, 2846, 2231, 1520, 1498, 1444, 1377, 1346, 1243, 1189, 1089, 1026, 983, 892, 776. δ_{H} (300 MHz, CDCl₃) 4.60 (d, *J* = 13 Hz, 2H, NCH₂), 4.10 (t, *J* = 7 Hz, 2H, CH₂OH), 3.30 (t, *J* = 13 Hz, 2H, NCH₂), 2.29 - 2.16 (m, 2H, CHCH₂), 2.16 - 2.05 (m, 1H, CH), 1.95 (s, 9H, CCH₃), 1.92 - 1.85 (m, 2H, CHCH₂), 1.80 (s, 1H, OH), 1.77 - 1.56 (m, 2H, CHCH₂). δ_{C} (75 MHz, CDCl₃) 153.17, 152.58, 125.26, 120.20, 114.34, 114.02, 60.06, 51.46, 48.80, 38.89, 32.28, 31.96, 29.82.

2,3,9,10,16,17-Hexakis(butoxycarbonyl)-23-(*tert*-butylsulfanyl)-24-(diethylamino)tetrapyrazinoporphyrazinato zinc (II) (**1Zn**)

Anhydrous zinc acetate (511 mg, 2.79 mmol) and compound **10** (200 mg, 0.69 mmol) were placed in an oven-dried round-bottom flask under argon atmosphere. Anhydrous pyridine (0.25 mL) was added, and the mixture was stirred at 160 °C for 15 min. Compound **6** (700 mg, 2.12 mmol) was dissolved in anhydrous pyridine (0.7 mL) and added to the mixture in two

equal portions within 15 min. The resulting mixture was refluxed for 3 h. The reaction mixture was cooled and poured into water (50 mL). The suspension was collected *via* filtration, washed thoroughly with water and air-dried. The target TPyzPz **1Zn** was isolated using column chromatography as the fifth intense green-blue fraction using chloroform/ethyl acetate/pyridine (10:3:1) as the eluent (*R_f* = 0.18). The product was purified *via* column chromatography once more using chloroform/THF (20:1) as the eluent and finally washed with hexane. Yield 6 mg (0.6 %) of green-blue solid. Found: C, 52.91; H, 5.48; N, 16.79. Calcd. for C₆₂H₇₃N₁₇O₁₂SZn + 4H₂O: C, 52.52; H, 5.76; N, 16.79 %. λ_{\max} (THF, 1 μM)/nm ($\epsilon/\text{dm}^3 \text{mol}^{-1} \text{cm}^{-1}$) 652 (116 960), 591 (sh), 371 (88 090). $\nu_{\max}/\text{cm}^{-1}$ 2962, 2874, 1731, 1629, 1551, 1345, 1244, 1208, 1177, 1086, 938, 762. δ_{H} (500 MHz, CDCl₃/pyridine-d₅) 4.76 (t, *J* = 6 Hz, 10H, OCH₂), 4.71 (t, *J* = 6 Hz, 2H, OCH₂), 4.06 (q, *J* = 6.4 Hz, 4H, NCH₂), 2.10 (s, 9H, CCH₃), 2.08 – 1.98 (m, 12H, CH₂), 1.84 – 1.63 (m, 12H, CH₂), 1.55 (t, *J* = 7 Hz, 6H, NCH₂CH₃), 1.23 – 1.07 (m, 18H, CH₂CH₃). δ_{C} (125 MHz, CDCl₃/pyridine-d₅) 165.43, 165.41, 165.37, 165.25, 165.04, 156.86, 156.20, 156.05, 153.90, 153.88, 151.90, 151.22, 149.98, 148.97, 148.88, 148.50, 147.03, 146.85, 146.49, 146.39, 146.36, 145.99, 145.81, 141.87, 67.17, 67.13, 67.12, 66.94, 51.01, 45.23, 30.97, 30.86, 30.77, 30.75, 30.74, 19.43, 19.40, 19.38, 14.05, 13.98, 13.94, 13.83. *m/z* (MALDI TOF) 1343.3 [M]⁺, 1366.3 [M + Na]⁺, 1382.3 [M + K]⁺. HRMS (ESI): *m/z* calcd. for C₆₂H₇₄N₁₇O₁₂SZn 1344.4710 [M + H]⁺, found 1344.4703.

General procedure for synthesis of metal-free TPyzPzs

Magnesium turnings (140 mg, 5.78 mmol) and a small crystal of iodine were refluxed in dry butanol (10 mL) for 3 h. Compound **12** (100 mg, 0.289 mmol, 1 eq.) and compound **7**, **8** or **9** (3 eq.) were added immediately in one portion, and the reflux was continued for 7 h. The mixture was cooled, and the solvent was removed under reduced pressure. An aqueous solution of acetic acid (50 % (v/v), 50 mL) was added, and the suspension was stirred for 1 h at room temperature. The dark solid was collected *via* filtration, washed with water and air-dried. The crude product was dissolved in THF (20 mL), and *p*-toluenesulfonic acid (550 mg, 2.89 mmol) was added to the solution followed by stirring at rt for 1 h. The mixture was poured into water, and the suspension was collected *via* filtration and washed with water. The product was purified *via* column chromatography on silica (eluents are mentioned below), and the second most intense green or blue-green fraction was collected. Finally, the product was washed with hexane.

2,3,9,10,16,17,23-Heptakis(*tert*-butylsulfanyl)-24-[4-(2-hydroxyethyl)piperidin-1-yl]tetrapyrazinoporphyrazine (**3H**)

Compound **3H** was prepared from compound **12** (100 mg, 0.289 mmol) and compound **7** (266 mg, 0.868 mmol) following the general procedure for the synthesis of metal-free TPyzPz. Mobile phase: chloroform/THF (20:1) (*R_f* = 0.5). Yield 32 mg (9 %) of dark green solid. Found: C, 55.65; H, 6.45; N, 18.51. Calcd. for: C₅₉H₇₉N₁₇OS₇: C, 55.94; H, 6.29; N, 18.80 %. λ_{\max}

(THF, 1 μM)/nm ($\epsilon/\text{dm}^3 \text{ mol}^{-1} \text{ cm}^{-1}$) 672 (159 890), 642 (127 840), 616 (47 580), 589 (33 330), 477 (61 460), 367 (141 460). $\nu_{\text{max}}/\text{cm}^{-1}$ 3302, 2960, 2919, 1637, 1521, 1477, 1456, 1398, 1231, 1140, 1087, 1023, 969, 765, 676. δ_{H} (300 MHz, $\text{CDCl}_3/\text{pyridine-d}_5$) 4.70 (d, $J = 12$ Hz, 2H, NCH_2), 4.04 (t, $J = 6$ Hz, 2H, CH_2OH), 3.52 (t, $J = 12$ Hz, 2H, NCH_2), 2.35 – 2.10 (m, 66H, $\text{CH}_3 + \text{CHCH}_2 + \text{CH}$), 2.02 – 1.83 (m, 4H, CHCH_2), -2.35 (s, 2H, NH). δ_{C} (75 MHz, $\text{CDCl}_3/\text{pyridine-d}_5$) 159.66, 159.60, 159.08, 158.61, 158.46, 158.21, 157.36, 156.32, 150.21, 148.75, 143.69, 143.40, 141.94, 140.66, 139.95, 59.63, 51.78, 51.53, 51.49, 51.42, 51.38, 50.55, 50.35, 40.10, 33.00, 32.73, 30.94, 30.84, 30.80, 30.74, 30.68, 30.63. HRMS (ESI): m/z calcd. for $\text{C}_{59}\text{H}_{80}\text{N}_{17}\text{OS}_7$ 1266.4771 $[\text{M} + \text{H}]^+$; found 1266.4777.

2-(*tert*-Butylsulfanyl)-3-[4-(2-hydroxyethyl)piperidin-1-yl]-9,10,16,17,23,24-hexaneopentyltetrapyrzinozopyrazine (4H)

Compound **4H** was prepared from compound **12** (100 mg, 0.289 mmol) and compound **8** (235 mg, 0.868 mmol) following the general procedure for the synthesis of metal-free TPzPz. Mobile phase: chloroform/THF/methanol (100:1:1) ($R_f = 0.42$). Yield 40 mg (12 %) of dark blue solid. Found: C, 66.24; H, 7.80; N, 19.82. Calcd. for $\text{C}_{65}\text{H}_{91}\text{N}_{17}\text{OS} + \text{H}_2\text{O}$: C, 66.35; H, 7.97; N, 20.24 %. λ_{max} (THF, 1 μM)/nm ($\epsilon/\text{dm}^3 \text{ mol}^{-1} \text{ cm}^{-1}$) 662 (125 430), 627 (88 590), 610 (sh), 580 (sh), 510 (22 940), 344 (105 750). $\nu_{\text{max}}/\text{cm}^{-1}$ 3302, 2953, 2867, 1658, 1572, 1478, 1452, 1363, 1282, 1229, 1137, 1045, 1024, 970, 887, 799, 721, 694. δ_{H} (300 MHz, $\text{CDCl}_3/\text{pyridine-d}_5$) 4.70 (d, $J = 12$ Hz, 2H, NCH_2), 3.98 (t, $J = 6$ Hz, 2H, CH_2OH), 3.74 (s, 4H, CCH_2), 3.67 (s, 4H, CCH_2), 3.64 (s, 2H, CCH_2), 3.62 (s, 2H, CCH_2), 3.43 (t, $J = 12$ Hz, 2H, NCH_2), 2.21 (s, 9H, CH_3), 2.18-2.13 (m, 3H, $\text{CHCH}_2 + \text{CH}$), 1.92 – 1.73 (m, 4H, CHCH_2), 1.47 (s, 9H, CH_3), 1.38 (s, 9H, CH_3), 1.37 – 1.29 (m, 36H, CH_3), -1.07 (s, 2H, NH). δ_{C} (75 MHz, $\text{CDCl}_3/\text{pyridine-d}_5$) 160.17, 158.35, 158.05, 157.93, 157.90, 157.77, 157.68, 148.50, 148.33, 148.18, 143.38, 143.29, 141.23, 138.89, 59.61, 51.22, 50.42, 48.35, 48.20, 48.10, 47.95, 47.89, 39.90, 34.77, 34.73, 34.60, 34.58, 34.30, 32.84, 32.62, 30.67, 30.40, 30.33. HRMS (ESI): m/z calcd. for $\text{C}_{65}\text{H}_{92}\text{N}_{17}\text{OS}$ 1158.7386 $[\text{M} + \text{H}]^+$; found 1158.7391.

2,3,9,10,16,17-Hexabutoxy-23-(*tert*-butylsulfanyl)-24-[4-(2-hydroxyethyl)piperidin-1-yl]tetrapyrzinozopyrazine (5H)

Compound **5H** was prepared from compound **12** (100 mg, 0.289 mmol) and compound **9** (238 mg, 0.868 mmol) following the general procedure for the synthesis of metal-free TPzPz. Mobile phase: chloroform/THF (10:1) ($R_f = 0.25$). Yield 55 mg (16 %) of dark blue-green solid. Found: C, 58.82; H, 6.68; N, 19.44. Calcd. for $\text{C}_{59}\text{H}_{79}\text{N}_{17}\text{O}_7\text{S} + 2\text{H}_2\text{O}$: C, 58.74; H, 6.93; N, 19.74 %. λ_{max} (THF, 1 μM)/nm ($\epsilon/\text{dm}^3 \text{ mol}^{-1} \text{ cm}^{-1}$) 650 (123 950), 612 (91 770), 599 (sh), 562 (26 670), 428 (45 580), 349 (111 260). $\nu_{\text{max}}/\text{cm}^{-1}$ 3298, 2960, 2933, 2873, 1844, 1636, 1576, 1558, 1473, 1456, 1446, 1379, 1314, 1249, 1144, 1061, 1020, 968, 927, 782, 742. δ_{H} (500 MHz, $\text{CDCl}_3/\text{pyridine-d}_5$) 5.59 (br s, 1H, OH), 5.19 (t, $J = 7$ Hz, 2H, OCH_2), 5.15 – 5.08 (m, 2H, OCH_2), 4.99 – 4.93 (m, 2H, OCH_2), 4.92 – 4.77 (m, 6H, OCH_2),

4.55 (d, $J = 12$ Hz, 2H, NCH_2), 4.10 – 4.07 (m, 2H, CH_2OH , overlapped by signal of water), 3.55 (t, $J = 12$ Hz, 2H, NCH_2), 2.42 – 2.13 (m, 24H, $\text{CH}_3 + \text{CHCH}_2 + \text{CH}$), 2.03 – 1.82 (m, 16H, $\text{CHCH}_2 + \text{CH}$), 1.40 – 1.25 (m, 18H, CH_3). δ_{C} (125 MHz, $\text{CDCl}_3/\text{pyridine-d}_5$) 157.43, 155.47, 153.18, 153.06, 152.67, 152.62, 142.94, 141.58, 139.01, 138.25, 137.87, 68.66, 68.60, 68.48, 68.37, 68.31, 68.17, 59.84, 50.69, 50.23, 40.28, 32.97, 32.90, 31.41, 31.35, 31.29, 31.24, 31.00, 19.89, 19.84, 19.82, 19.80, 14.44, 14.42, 14.40, 14.38, 14.35. HRMS (ESI): m/z calcd. for $\text{C}_{59}\text{H}_{80}\text{N}_{17}\text{O}_7\text{S}$ 1170.6142 $[\text{M} + \text{H}]^+$; found 1170.6147.

General procedure for synthesis of zinc TPzPzs

The metal-free derivative (1 eq) was dissolved in pyridine (15 mL), and anhydrous zinc acetate (7 eq.) was added. The mixture was refluxed for 90 min. The solution was concentrated under reduced pressure, and water (50 mL) was added. The resulting suspension was collected *via* filtration, thoroughly washed with water and air-dried. The product was purified using column chromatography on silica (used eluents are mentioned below) and finally washed with hexane.

2,9,10,16,17,23,24-Heptakis(*tert*-butylsulfanyl)-3-[4-(2-hydroxyethyl)piperidin-1-yl]tetrapyrzinozopyrazinato zinc (II) (3Zn)

Compound **3Zn** was prepared from **3H** (50 mg, 0.04 mmol) following the general procedure for the synthesis of zinc TPzPz. Mobile phase: chloroform/THF (10:1) ($R_f = 0.45$). Yield 45 mg (93 %) of dark green solid. Found: C, 53.56; H, 5.73; N, 17.21. Calcd. for $\text{C}_{59}\text{H}_{77}\text{N}_{17}\text{OS}_7\text{Zn}$: C, 53.27; H, 5.83; N, 17.60 %. λ_{max} (THF, 1 μM)/nm ($\epsilon/\text{dm}^3 \text{ mol}^{-1} \text{ cm}^{-1}$) 650 (290 470), 622 (sh), 590 (41 200), 470 (sh), 376 (161 680). $\nu_{\text{max}}/\text{cm}^{-1}$ 2959, 2918, 1683, 1558, 1362, 1256, 1233, 1143, 1098, 1055, 976, 846, 781, 748. δ_{H} (300 MHz, $\text{CDCl}_3/\text{pyridine-d}_5$) 4.58 (d, $J = 12$ Hz, 2H, NCH_2), 3.99 (t, $J = 6$ Hz, 2H, CH_2OH), 3.46 (t, $J = 12$ Hz, 2H, NCH_2), 2.39 – 2.12 (m, 65H, $\text{CH}_3 + \text{CHCH}_2$), 2.09 – 1.97 (m, 1H, CH), 1.94 – 1.79 (m, 4H, CHCH_2). δ_{C} (75 MHz, $\text{CDCl}_3/\text{pyridine-d}_5$) 159.01, 158.40, 158.34, 157.99, 157.24, 155.18, 152.00, 151.68, 151.32, 151.21, 150.94, 150.82, 144.75, 144.60, 144.58, 144.46, 144.44, 143.34, 136.01, 123.83, 59.61, 51.47, 51.46, 51.43, 51.39, 51.33, 50.46, 50.18, 40.09, 32.90, 32.67, 31.01, 30.93, 30.85, 30.80. m/z (MALDI TOF) 1327.2, $[\text{M}]^+$; 1350.2 $[\text{M} + \text{Na}]^+$; 1366.2 $[\text{M} + \text{K}]^+$. HRMS (ESI): m/z calcd. for $\text{C}_{59}\text{H}_{78}\text{N}_{17}\text{OS}_7\text{Zn}$ 1328.3906 $[\text{M} + \text{H}]^+$; found 1328.3912.

2-(*tert*-Butylsulfanyl)-3-[4-(2-hydroxyethyl)piperidin-1-yl]-9,10,16,17,23,24-hexaneopentyltetrapyrzinozopyrazinato zinc (4Zn)

Compound **4Zn** was prepared from **4H** (50 mg, 0.043 mmol) following the general procedure for the synthesis of zinc TPzPz. Mobile phase: chloroform/THF (10:1) ($R_f = 0.40$). Yield 29 mg (55 %) of dark blue solid. Found: C, 61.20; H, 7.13; N, 18.32. Calcd. for $\text{C}_{65}\text{H}_{89}\text{N}_{17}\text{OSZn} + 3\text{H}_2\text{O}$: C, 61.18; H, 7.50; N, 18.66 %. λ_{max} (THF, 1 μM)/nm ($\epsilon/\text{dm}^3 \text{ mol}^{-1} \text{ cm}^{-1}$) 639 (227 010), 610 (sh), 582 (33 180), 496 (sh), 357 (126 700).

$\nu_{\max}/\text{cm}^{-1}$ 2953, 2867, 1637, 1545, 1476, 1444, 1364, 1279, 1238, 1202, 1133, 1095, 1048, 1025, 983, 925, 860, 776. δ_{H} (300 MHz, $\text{CDCl}_3/\text{pyridine-d}_5$) 4.54 – 4.48 (m, 2H, NCH_2) 3.98 (t, $J = 7$ Hz, 2H, CH_2OH), 3.69 (s, 8H, CCH_2), 3.65 (s, 2H, CCH_2), 3.63 (s, 2H, CCH_2), 3.41 (t, $J = 12$ Hz, 2H, NCH_2), 2.26 – 2.11 (s, 11H, $\text{CH}_3 + \text{CHCH}_2$), 2.11–1.97 (m, 1H, CH) 1.92 – 1.74 (m, 4H, CHCH_2), 1.47 (s, 9H, CCH_3), 1.40 (s, 9H, CCH_3), 1.37 (s, 9H, CCH_3), 1.36 (s, 9H, CCH_3), 1.35 (s, 9H, CCH_3), 1.34 (s, 9H, CCH_3). δ_{C} (75 MHz, $\text{CDCl}_3/\text{pyridine-d}_5$) 158.13, 157.79, 157.71, 157.61, 157.49, 155.67, 152.39, 152.27, 151.96, 151.64, 151.30, 150.98, 147.70, 147.54, 147.50, 147.42, 147.40, 144.60, 143.29, 59.68, 50.58, 50.39, 48.26, 48.17, 48.03, 47.95, 40.01, 34.58, 34.29, 32.82, 32.67, 30.84, 30.46, 30.41, 30.36. m/z (MALDI TOF) 1219.5 $[\text{M}]^+$; 1242.5 $[\text{M} + \text{Na}]^+$; 1258.4 $[\text{M} + \text{K}]^+$. HRMS (ESI): m/z calcd. for $\text{C}_{65}\text{H}_{90}\text{N}_{17}\text{OSZn}$ 1220.6521 $[\text{M} + \text{H}]^+$; found 1220.6526.

2,3,9,10,16,17-Hexabutoxy-23-(tert-butylsulfanyl)-24-[4-(2-hydroxyethyl)piperidin-1-yl]tetrapyrrozinoporphyrazinato zinc (5Zn)

Compound **5Zn** was prepared from **5H** (30 mg, 0.026 mmol) following the general procedure for the synthesis of zinc TPyzPz. Mobile phase: chloroform/THF (10:1) ($R_f = 0.42$). Yield 28 mg (88 %) of dark blue-green solid. Found: C, 55.32; H, 6.28; N, 18.25. Calcd. for $\text{C}_{59}\text{H}_{77}\text{N}_{17}\text{O}_7\text{SZn} + 3\text{H}_2\text{O}$: C, 55.03; H, 6.50; N, 18.49 %. λ_{\max} (THF, 1 μM)/nm ($\epsilon/\text{dm}^3 \text{mol}^{-1} \text{cm}^{-1}$) 626 (239 430), 601 (sh), 569 (32 610), 418 (sh), 361 (132 790). $\nu_{\max}/\text{cm}^{-1}$ 2961, 2873, 1653, 1541, 1507, 1441, 1378, 1306, 1251, 1118, 1059, 1026, 970, 935, 827, 745. δ_{H} (500 MHz, $\text{CDCl}_3/\text{pyridine-d}_5$) 5.23 (t, $J = 7$ Hz, 2H, OCH_2), 5.17 – 4.92 (m, 10H, OCH_2), 4.46 (d, $J = 12$ Hz, 2H, NCH_2), 3.98 (t, $J = 6$ Hz, 2H, CH_2OH), 3.38 (t, $J = 12$ Hz, 2H, NCH_2), 2.41 – 1.96 (m, 24H, $\text{SCCH}_3 + \text{CHCH}_2 + \text{CH}_2\text{CH}_2\text{CH}_3 + \text{CH}$), 1.93 – 1.66 (m, 16H, $\text{CH}_2\text{CH}_2\text{CH}_3$), 1.31 – 1.12 (m, 18H, CH_2CH_3). δ_{C} (125 MHz, $\text{CDCl}_3/\text{pyridine-d}_5$) 157.40, 155.11, 152.82, 152.80, 152.75, 151.31, 151.16, 150.83, 150.42, 144.59, 143.54, 141.56, 141.46, 141.23, 141.21, 68.25, 68.05, 59.71, 50.61, 49.97, 40.09, 32.81, 32.73, 31.18, 31.12, 31.02, 19.65, 14.19. m/z (MALDI TOF) 1231.4 $[\text{M}]^+$; 1254.3 $[\text{M} + \text{Na}]^+$; 1270.3 $[\text{M} + \text{K}]^+$. HRMS (ESI): m/z calcd. for $\text{C}_{59}\text{H}_{78}\text{N}_{17}\text{O}_7\text{SZn}$ 1232.5277 $[\text{M} + \text{H}]^+$; found 1232.5282.

Fluorescence measurements

All of the samples were repurified using preparative TLC prior to the photophysical measurements (both Φ_{F} and Φ_{Δ}) to ensure that they were highly pure. The fluorescence spectra were obtained using an AMINCO Bowman Series 2 luminescence spectrometer. All of the emission spectra were corrected for the instrument response. The fluorescence quantum yields (Φ_{F}) were determined in THF *via* the comparative method using unsubstituted zinc phthalocyanine (ZnPc, Sigma-Aldrich) as a reference ($\Phi_{\text{F}} = 0.32$ in THF^5). Both the reference and sample were excited at 600 nm. The absorbance at the excitation wavelength was maintained below 0.015, and the absorbance at the Q-band maximum was maintained below 0.05 to limit the inner filter effect. The value of Φ_{F} was calculated using Eq. 1³⁸:

$$\Phi_{\text{F}}^{\text{S}} = \Phi_{\text{F}}^{\text{R}} \frac{F^{\text{S}}}{F^{\text{R}}} \left(\frac{1 - 10^{-A^{\text{R}}}}{1 - 10^{-A^{\text{S}}}} \right) \quad (\text{Eq. 1})$$

where F is the integrated area under the emission spectrum and A is the absorbance at the excitation wavelength. The superscripts R and S correspond to the reference and sample, respectively. All of the experiments were performed in triplicate with the reported data representing the mean (estimated error $\pm 15\%$).

Determination of the singlet oxygen production

The quantum yields of the singlet oxygen (Φ_{Δ}) were determined in THF according to a previously published procedure³⁹ using the decomposition of a chemical trap 1,3-diphenylisobenzofuran (DPBF) with ZnPc as a reference ($\Phi_{\Delta} = 0.53$ in THF^{25}). The detailed procedure was as follows: 2.5 mL of a DPBF stock solution in THF (5×10^{-5} M) was transferred into a 10 mm \times 10 mm quartz optical cell and saturated with oxygen for 1 min. Then, a stock solution of the tested compound in THF (typically 20 μL) was added to achieve an absorbance of the final solution in the Q-band maximum of approximately 0.1. The solution was stirred and irradiated using a xenon lamp (100 W, ozone-free XE DC short-arc lamp, Newport). The incident light was filtered through a water filter (6 cm) and an OG530 cut-off filter (Newport) to remove the heat and light below 523 nm, respectively. A decrease of DPBF in the solution as a function of the irradiation time was monitored at 414 nm. All of the experiments were performed in triplicate, and the data presented herein represents the mean of the three experiments (estimated error: $\pm 15\%$).

Electrochemistry

The electrochemical measurements (i.e., cyclic voltammetry and square wave voltammetry) were performed at room temperature using an Autolab PGSTAT101 potentiostat. The measurements were carried out with a three electrode setup consisting of a Pt working electrode, a Pt counter electrode, and an Ag/AgCl reference electrode separated from the bulk solution by an integrated salt bridge. The detailed procedure was as follows: a 0.1 M solution of tetrabutylammonium hexafluorophosphate in dry THF (5 mL), which was the supporting electrolyte, was added to the cell and bubbled with nitrogen for 5 minutes to remove the residual oxygen. Next, the appropriate compound (10 mg) was added and bubbling was continued for the next 5 minutes. Half – wave potentials ($E_{1/2}$) were recorded from square wave voltammetry with potential step of 5 mV and a scan rate of 100 mV/s. The obtained data listed in Table 1 were referenced to SCE with ferrocene as an internal standard ($E_{1/2}(\text{Fc}/\text{Fc}^+) = 0.56$ V vs SCE).⁴⁰

Protonation of nitrogens

The stock solution (2 mL) of the tested compound in dimethylsulfoxide ($c = 1 \mu\text{M}$) was transferred into the quartz optical cell (10 \times 10 mm). The absorption and emission spectra ($\lambda_{\text{exc}} = 595$ nm) were measured after addition of defined

amount of concentrated sulfuric acid into the sample in range from 0% to 41 % (v/v). The fluorescence emission spectra were corrected for instrument response. Absorption spectra presented in ESI (Figure S5) were corrected for dilution.

Acknowledgements

This work was supported by Grant Agency of Charles University (GA UK 1182313/2013) and Czech Science Foundation (No. 14-02165P). The authors thank Jiří Kuneš for the NMR measurements, Juraj Lenčo for the MALDI TOF MS measurements and Lucie Nováková for the HR MS measurement.

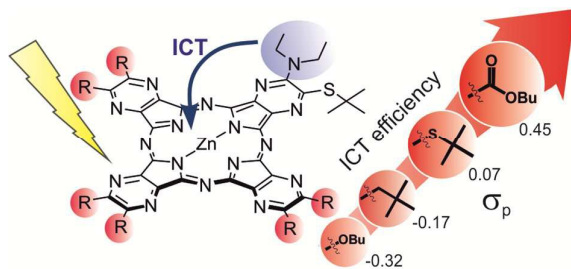
Notes and references

^a Department of Pharmaceutical Chemistry and Drug Control, Faculty of Pharmacy in Hradec Kralove, Charles University in Prague, Heyrovského 1203, 50005, Hradec Kralove, Czech Republic. E-mail: petr.zimcik@faf.cuni.cz; Fax: +420 495067167; Tel: +420 495067257

^b Department of Biophysics and Physical Chemistry, Faculty of Pharmacy in Hradec Kralove, Charles University in Prague, Heyrovského 1203, 50005 Hradec Kralove, Czech Republic. E-mail: veronika.novakova@faf.cuni.cz; Fax: +420 495067167; Tel: +420 495067380

† Electronic Supplementary Information (ESI) available: [Absorption, emission, excitation spectra of prepared compounds, NMR spectra]. See DOI: 10.1039/b000000x/

- R. P. Linstead, E. G. Noble and J. M. Wright, *J. Chem. Soc.*, 1937, 911-921.
- E. H. Mørkved, N. K. Afseth and P. Zimcik, *J. Porphyrins Phthalocyanines*, 2007, **11**, 130-138.
- S. V. Kudrevich and J. E. vanLier, *Coord. Chem. Rev.*, 1996, **156**, 163-182.
- M. P. Donzello, E. Viola, X. H. Cai, L. Mannina, C. Ercolani and K. M. Kadish, *Inorg. Chem.*, 2010, **49**, 2447-2456.
- P. Zimcik, V. Novakova, K. Kopecky, M. Miletin, R. Z. Uslu Kobak, E. Svandrlíkova, L. Váchová and K. Lang, *Inorg. Chem.*, 2012, **51**, 4215-4223.
- P. Zimcik, M. Miletin, H. Radilova, V. Novakova, K. Kopecky, J. Svec and E. Rudolf, *Photochem. Photobiol.*, 2010, **86**, 168-175.
- E. A. Vlasova, N. Hessenauer-Ilicheva, D. S. Salnikov, E. V. Kudrik, S. V. Makarov and R. van Eldik, *Dalton Trans.*, 2009, **0**, 10541-10549.
- M. P. Donzello, Z. Ou, D. Dini, M. Meneghetti, C. Ercolani and K. M. Kadish, *Inorg. Chem.*, 2004, **43**, 8637-8648.
- S. V. Efimova, O. I. Koifman, V. V. Bykova, I. Y. Lukyanov, V. V. Sotsky and N. V. Usoltseva, *Mol. Cryst. Liq. Cryst.*, 2012, **553**, 66-71.
- N. B. McKeown, S. Makhseed, K. J. Msayib, L. L. Ooi, M. Helliwell and J. E. Warren, *Angew. Chem., Int. Ed.*, 2005, **44**, 7546-7549.
- L. Vachova, V. Novakova, K. Kopecky, M. Miletina and P. Zimcik, *Dalton Trans.*, 2012, **41**, 11651-11656.
- V. Novakova, P. Zimcik, M. Miletin, L. Vachova, K. Kopecky, K. Lang, P. Chábera and T. Polivka, *Phys. Chem. Chem. Phys.*, 2010, **12**, 2555-2563.
- V. Novakova, M. Miletin, K. Kopecky and P. Zimcik, *Chem. Eur. J.*, 2011, **17**, 14273-14282.
- V. Novakova, L. Lochman, I. Zajícová, K. Kopecky, M. Miletin, K. Lang, K. Kirakci and P. Zimcik, *Chem. Eur. J.*, 2013, **19**, 5025-5028.
- V. Novakova, P. Hladik, T. Filandrova, I. Zajícova, V. Krepsova, M. Miletin, J. Lenco and P. Zimcik, *Phys. Chem. Chem. Phys.*, 2014, **16**, 5440-5446.
- C. Hansch, A. Leo and R. W. Taft, *Chem. Rev.*, 1991, **91**, 165-195.
- Z. Musil, P. Zimcik, M. Miletin, K. Kopecky, P. Petrik and J. Lenco, *J. Photochem. Photobiol., A*, 2007, **186**, 316-322.
- P. Zimcik, M. Miletin, M. Kostka, J. Schwarz, Z. Musil, K. Kopecky, *J. Photochem. Photobiol., A*, 2004, **163**, 21-28.
- P. Zimcik, M. Miletin, V. Novakova, K. Kopecky, M. Nejedla, V. Stara and K. Sedlackova, *Aust. J. Chem.*, 2009, **62**, 425-433.
- V. Novakova, P. Zimcik, M. Miletin, K. Kopecky and Z. Musil, *Eur. J. Org. Chem.*, 2010, **2010**, 732-739.
- A. Y. Tolbin, V. E. Pushkarev, I. O. Balashova, A. V. Dzuban, P. A. Tarakanov, S. A. Trashin, L. G. Tomilova and N. S. Zefirov, *New J. Chem.*, 2014, **38**, 5825-5831.
- A. Y. Tolbin, V. E. Pushkarev, V. B. Sheinin, S. A. Shabunin and L. G. Tomilova, *J. Porphyrins Phthalocyanines*, 2014, **18**, 155-161.
- T. Fukuda, N. Kobayashi, in *Handbook of Porphyrin Science* ed. K. M. Kadish, Smith K. M., Guillard R., World Scientific Publishing, Singapore, 2010, vol. 9.
- F. Mitzel, S. FitzGerald, A. Beeby and R. Faust, *Eur. J. Org. Chem.*, 2004, 1136-1142.
- L. Kaestner, M. Cesson, K. Kassab, T. Christensen, P. D. Edminson, M. J. Cook, I. Chambrier and G. Jori, *Photochem. Photobiol. Sci.*, 2003, **2**, 660-667.
- M. Durmus, H. Yaman, C. Göl, V. Ahsen, T. Nyokong, *Dyes Pigm.*, 2011, **91**, 153-163.
- M. P. Donzello, E. Viola, C. Bergami, D. Dini, C. Ercolani, M. Giustini, K. M. Kadish, M. Meneghetti, F. Monacelli, A. Rosa and G. Ricciardi, *Inorg. Chem.*, 2008, **47**, 8757-8766.
- R. W. Redmond and J. N. Gamlin, *Photochem. Photobiol.*, 1999, **70**, 391-475.
- S. Makhseed, M. Machacek, W. Alfadly, A. Tuhl, M. Vinodh, T. Simunek, V. Novakova, P. Kubat, E. Rudolf and P. Zimcik, *Chem. Commun.*, 2013, **49**, 11149-11151.
- J.-Y. Chen, A. Ogunsiye and T. Nyokong, *New J. Chem.*, 2004, **28**, 822-827.
- A. Tuhl, S. Makhseed, P. Zimcik, N. Al-Awadi, V. Novakova and J. Samuel, *J. Porphyrins Phthalocyanines*, 2012, **16**, 817-825.
- J. Svec, P. Zimcik, L. Novakova, O. A. Rakitin, S. A. Amelichev, P. A. Stuzhin and V. Novakova, *European Journal of Organic Chemistry*, 2015, **2015**, 596-604.
- Y. Urano, D. Asanuma, Y. Hama, Y. Koyama, T. Barrett, M. Kamiya, T. Nagano, T. Watanabe, A. Hasegawa, P. L. Choyke and H. Kobayashi, *Nat. Med.*, 2009, **15**, 104-109.
- X. J. Jiang, P. C. Lo, S. L. Yeung, W. P. Fong and D. K. P. Ng, *Chem. Commun.*, 2010, **46**, 3188-3190.
- A. Beeby, S. FitzGerald and C. F. Stanley, *J. Chem. Soc., Perkin Trans. 2*, 2001, 1978-1982.
- V. Novakova, E. H. Mørkved, M. Miletin and P. Zimcik, *J. Porphyrins Phthalocyanines*, 2010, **14**, 582-591.
- L. Fajari, P. Fors, K. Lang, S. Nonell and F. R. Trull, *J. Photochem. Photobiol., A*, 1996, **93**, 119-128.
- J. R. Lakowicz, *Principles of fluorescence spectroscopy*, 3rd edn., Springer, New York, 2006.
- Z. Musil, P. Zimcik, M. Miletin, K. Kopecky, M. Link, P. Petrik and J. Schwarz, *J. Porphyrins Phthalocyanines*, 2006, **10**, 122-131.
- N. G. Connelly and W. E. Geiger, *Chem. Rev.*, 1996, **96**, 877-910.



TOC text:

Efficiency of intramolecular charge transfer correlates with Hammett constants of peripheral substituents and the first reduction potential of tetrapyrrozinoporphyrazines.